

# Dynamic viscoelastic properties of carboxymethylcellulose during isothermal water sorption

Shoichiro Yano

National Institute of Materials and Chemical Research, 1-1 Higashi, Tsukuba-shi, Ibaraki 305, Japan

(Received 16 March 1992; revised 21 September 1992)

The dynamic viscoelastic properties of carboxymethylcellulose sodium salt (NaCMC) were measured isothermally as a function of relative humidity (r.h.). The dynamic modulus decreased with increasing r.h. and dropped markedly at about 70% r.h. In the  $\tan \delta$  curve, a small peak appeared at about 20–30% r.h. and a large peak was observed at 80% r.h. To study the mechanism of these relaxations, the dynamic modulus was measured isothermally as a function of time at constant r.h. and the data were analysed in terms of the kinetics. Below about 70% r.h. bound water may be formed, having an activation energy of 15.0–15.6 kJ mol<sup>-1</sup>. On the other hand, above 70% r.h., two types of mechanism may occur simultaneously: formation of bound water around hydrophilic groups with activation energy of 15.6 kJ mol<sup>-1</sup>, and formation of free water with activation energy of 13.0 kJ mol<sup>-1</sup>. Consequently, the  $\tan \delta$  peak occurring at about 20–30% r.h. may be caused by the onset of local molecular motion of the hydrophilic groups, and the peak at about 80% r.h. by the onset of micro-Brownian motion of chain molecules plasticized with free water.

(Keywords: carboxymethylcellulose sodium salt; dynamic viscoelasticity; water sorption; sorption isotherm; glass transition concentration; molecular motion)

## INTRODUCTION

The dynamic modulus,  $E'$ , of polymeric materials decreases with increasing temperature and drastically drops at the glass transition temperature,  $T_g$ , at which a peak in  $\tan \delta$  occurs. This marked change in the dynamic viscoelasticity is caused by the micro-Brownian motion of the polymer chains. In the case of hydrophilic polymers, however, micro-Brownian motion can also occur during isothermal water sorption. In a previous report<sup>1</sup>, the dynamic viscoelasticity of regenerated cellulose was measured as a function of relative humidity (r.h.) at constant temperatures of 30, 50 and 80°C. The dynamic modulus,  $E'$ , decreased rapidly at about 70–80% r.h. and a peak appeared in the  $\tan \delta$  curves. We also observed this kind of transition, measured by using torsional braid analysis, in lignosulfonates<sup>2,3</sup>. A peak in the logarithmic decrement,  $\Delta$ , shifted to a higher r.h. region when molecular weights of lignosulfonates increased<sup>2</sup>. The peak in the  $\Delta$  curve of lignosulfonates with a larger counterion radius occurred at a lower r.h.<sup>3</sup>. Lewis and Tobin measured the dynamic viscoelasticity of poly(methyl methacrylate) (PMMA)–benzene<sup>4</sup> and polystyrene (PSt)–benzene<sup>5</sup> systems as a function of solvent concentration. A significant drop in the modulus and a peak in the  $\Delta$  curve were observed during desorption of the solvent. This transition was named the glass transition concentration,  $C_g$ , at which micro-Brownian motion occurs.

In the present study, the dynamic viscoelastic properties of hygroscopic carboxymethylcellulose sodium salt (NaCMC) were measured isothermally as a function of r.h. For the kinetic analysis, the dynamic viscoelastic properties of NaCMC were also measured as a function

of time at constant temperatures and r.h. The effect of water sorption on the viscoelastic properties of NaCMC was investigated from the view point of kinetics.

## EXPERIMENTAL

The specimen used in this study was NaCMC with a degree of substitution of 0.6, obtained from Wako Pure Chemical Industries, Ltd.

The dynamic viscoelastic properties of NaCMC during water sorption were measured using a Rheovibron DDV-IIC (Orientec Co., Ltd) connected to a moisture generator<sup>2</sup>. R.h. was controlled at 16–100% at 30°C, and 5–100% at 50 and 80°C. The dynamic modulus and  $\tan \delta$  were measured as a function of r.h. at 30, 50 and 80°C at 110 Hz.

It is difficult to obtain free-standing films of NaCMC, especially at high r.h. In order to measure the dynamic viscoelastic properties of NaCMC over a wide range of r.h., a ring-spring, as shown in *Figure 1*, was used as a support for NaCMC<sup>6</sup>. The ring-spring was made of

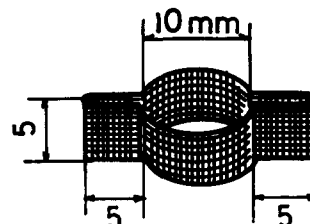


Figure 1 A ring-spring support made of stainless steel mesh for NaCMC

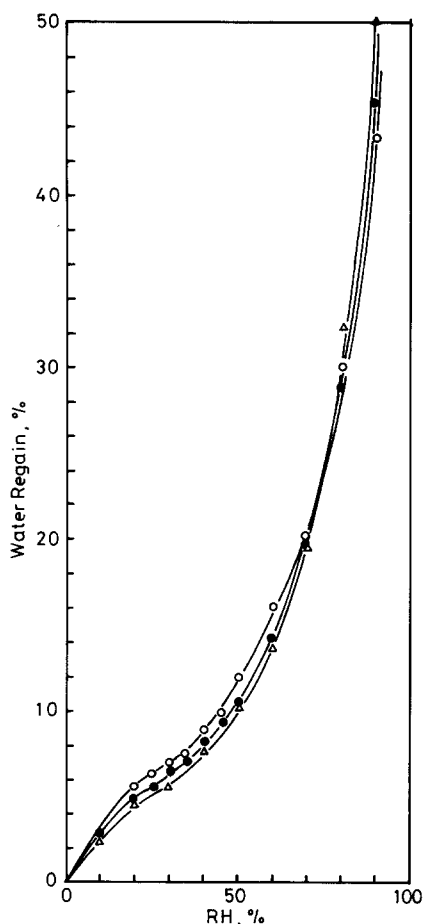


Figure 2 Sorption isotherms of NaCMC at 30 (○), 50 (●) and 80°C (△)

stainless mesh (100 mesh) and had a radius and height of 5 mm. The ring-spring was immersed in an aqueous polymer solution and dried. NaCMC was deposited on the ring-spring and fixed in the mesh. The necessary amount of polymer on the spring was 20–25% of the total weight of the specimen. The dynamic modulus was indicated as the relative value,  $E'_r$ , which was obtained by dividing the modulus,  $E'$ , at any r.h. by the initial value at r.h.=0 (dry state).

For the kinetic analysis, the dynamic modulus and  $\tan \delta$  were measured isothermally at constant r.h. as a function of time. Prior to measuring the dynamic viscoelasticity, the composite specimen, consisting of NaCMC and ring-spring, was dried at room temperature for 1 week and then at 70°C for 3 days *in vacuo* (about  $10^{-3}$  mmHg). The dried specimen was placed in a chamber of the dynamic viscoelastic apparatus which was maintained at a constant temperature of 30, 40, 50 or 60°C. A three-way tap was then turned to connect the chamber to the moisture generator maintained at a constant r.h. At this moment, time was determined as  $t=0$  and the dynamic viscoelasticity was measured as a function of elapsed time.

Sorption isotherms were measured at 30, 50 and 80°C using a quartz spring hung in a moisture-controlled chamber.

## RESULTS AND DISCUSSION

Figure 2 shows sorption isotherms of NaCMC at 30, 50 and 80°C. At less than 60% r.h., water

regain (weight of absorbed water  $\times$  100/weight of dry sample) was dependent upon the temperature. The water regain at higher temperatures was less than that at lower temperatures. This behaviour indicates an exothermic sorption process commonly observed in cellulosic materials<sup>1</sup>. Above 60% r.h. the water regain increased sharply with r.h., and the temperature dependence of the water regain was less prominent.

Figure 3 shows the dynamic viscoelastic properties of NaCMC as a function of r.h. at 30, 50 and 80°C. The modulus decreased gradually with increasing r.h., and at about 70% r.h. it decreased markedly, corresponding to the change in sorption isotherm. In the  $\tan \delta$  curve, a large peak appeared at about 80% r.h. The peak position was dependent upon the temperature, namely at a higher temperature the peak appeared at a lower r.h. This  $\tan \delta$  peak has also been observed in the case of regenerated cellulose<sup>1</sup> and lignosulfonates<sup>2,3</sup> during water sorption. This kind of  $\tan \delta$  peak also appeared during desorption of solvent for PMMA–benzene<sup>4</sup> and PSt–benzene<sup>5</sup> systems. This  $\tan \delta$  peak occurred as a result of the onset of micro-Brownian motion caused by the sorption of water.

At the lower r.h. region, 20–30%, another small  $\tan \delta$  peak was observed at each temperature. The location of this peak also depended on the temperature. This small  $\tan \delta$  peak resembles a secondary relaxation peak commonly observed in the temperature dispersion of polymers. This kind of secondary peak was also observed in regenerated cellulose<sup>1</sup> at about 60% r.h. and in lignosulfonates<sup>2,3</sup> at 40–50% r.h.

The behaviour of sorbed water in hydrophilic polymers has been classified into three regions<sup>7–9</sup>.

*Region I.* A few water molecules are absorbed on hydrophilic groups and a monolayer of water molecules is formed. The molecular motion of water in this region is strongly restricted by the hydrophilic groups, and the correlation time,  $\tau_c$ , has been calculated as  $10^{-5}$ – $10^{-7}$  s.

*Region II.* Multilayers of water molecules are formed

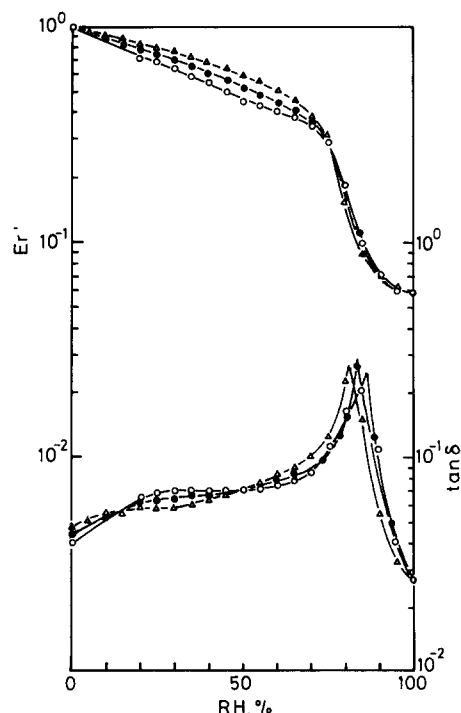
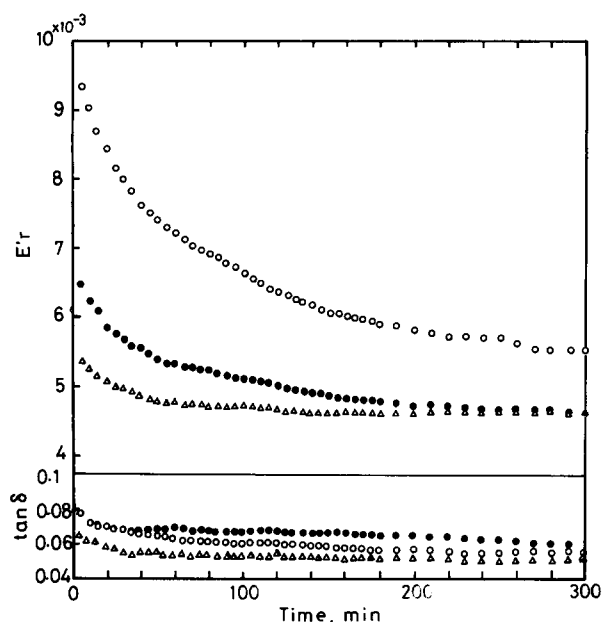


Figure 3 Dynamic viscoelastic properties of NaCMC as a function of r.h. at 30 (○), 50 (●) and 80°C (△)



**Figure 4** Dynamic viscoelastic properties of NaCMC as a function of time at 20% r.h. at 30 (○), 50 (●) and 60°C (△)

around hydrophilic polymers. In this region, water breaks intra- or intermolecular hydrogen bonds in the amorphous phase. The  $\tau_c$  value of water is on the order of  $10^{-7}$ – $10^{-9}$  s, and the molecular motion of water may be affected by the water around hydrophilic groups. Sorbed water in this region can be categorized as bound water.

**Region III.** Water molecules are absorbed in polymers as bulk water or free water. The molecular motion of water is not restricted by hydrophilic groups, and  $\tau_c$  is calculated as  $10^{-9}$ – $10^{-12}$  s. In this region, hydrophilic polymers are plasticized by water, and the molecular motion of the polymers is accelerated.

The  $\tan \delta$  peak and steep decrease in modulus at around 70–80% r.h. may be caused by plasticization of polymer molecules with free water, as in region III. Micro-Brownian motion of NaCMC may begin at around 70–80% r.h. due to formation of free water. On the other hand, at 20–30% r.h. a small amount of water (about 6 wt%) was absorbed, as can be seen in Figure 2, and water molecules surround the hydrophilic groups, as in region II. In this region, local mode motion of the hydrophilic groups may occur, causing the small  $\tan \delta$  peak at around 20–30% r.h.

In order to examine the mechanism of water absorption relating to the changes in the dynamic viscoelasticity, kinetic analysis was carried out. Figure 4 shows the changes in the dynamic viscoelastic properties of NaCMC at constant r.h. of 20%, at 30, 50 and 60°C, as a function of time. The dynamic modulus is expressed as a relative value,  $E_r'$ . The dynamic modulus,  $E'$  (in Pa), was measured using the Rheovibron DDV-IIC and calculated according to equation (1):

$$E' = (2 \times 10^{-8}/D)(S/L) \cos \delta \quad (1)$$

where  $D$  is the reading on a dynamic force dial of the Rheovibron apparatus,  $S$  is the cross-sectional area of the sample and  $L$  is the length of the sample. The  $\cos \delta$  value was converted from the reading on a  $\tan \delta$  meter of the apparatus. As every measurement was carried out using the same sample, the value  $S/L$  is constant and the

relative dynamic modulus,  $E_r'$ , can be simply calculated using equation (2):

$$E_r' = \cos \delta / D \quad (2)$$

This relative dynamic modulus,  $E_r'$ , decreased with time and reached equilibrium at 270, 200 and 70 min at 30, 50 and 60°C, respectively. The  $\tan \delta$  decreased slightly with time. The rate of decrease in the modulus with time can be calculated assuming a first-order reaction equation as follows:

$$d(E_r' - E_r^\infty)/dt = -k(E_r' - E_r^\infty) \quad (3)$$

$$\ln(E_r' - E_r^\infty) = \ln(E_r^0 - E_r^\infty) - kt \quad (4)$$

$$(E_r' - E_r^\infty) = A \exp(-kt) \quad (5)$$

where  $t$  is time,  $E_r^0$  is  $E_r'$  at  $t=0$ ,  $E_r^\infty$  is the equilibrium value of  $E_r'$ , and  $k$  is a rate constant.

The term  $\ln(E_r' - E_r^\infty)$  was calculated from Figure 4 and plotted against time. The results are shown in Figure 5. Straight lines were obtained at 30, 50 and 60°C, from which the rate constant,  $k$ , was calculated as  $1.15 \times 10^{-2}$ ,  $1.45 \times 10^{-2}$  and  $2.05 \times 10^{-2} \text{ min}^{-1}$ , respectively.

Figure 6 shows the plots of  $\ln(E_r' - E_r^\infty)$  versus time at 40% r.h. at various temperatures. A straight line was obtained at each temperature, as was also found at 20% r.h. (Figure 5). From each straight line, the rate constant  $k$  was calculated as  $1.62 \times 10^{-2}$ ,  $1.88 \times 10^{-2}$ ,  $2.25 \times 10^{-2}$ , and  $2.70 \times 10^{-2} \text{ min}^{-1}$  at 30, 40, 50 and 60°C, respectively.

The dynamic viscoelastic behaviour above 70% r.h. was considerably different from that below 70% r.h., as can be seen in Figure 3. The dynamic viscoelastic properties of NaCMC at a high r.h. of 80% were also measured as a function of time at 30, 50 and 60°C, as shown in Figure 7. The modulus,  $E_r'$ , decreased markedly with time and reached equilibrium at 200, 140 and 70 min at 30, 50 and 60°C, respectively. The  $\tan \delta$  curves were quite different from those at 20% r.h. A large  $\tan \delta$  peak appeared at 90, 60 and 50 min at 30, 50 and 60°C, respectively.

The decrease in the modulus was plotted according to equation (4), as shown in Figure 8. A plot of  $\ln(E_r' - E_r^\infty)$  versus time approached a straight line above a certain time,  $t_m$ . Values of  $t_m$  were 90, 60 and 50 min at 30, 50

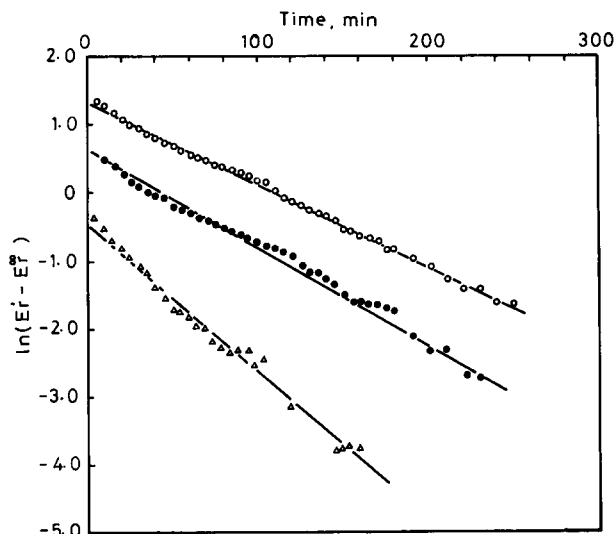


**Figure 5** Plot of  $\ln(E_r' - E_r^\infty)$  versus time at 30 (○), 50 (●) and 60°C (△) at 20% r.h. according to equation (5)

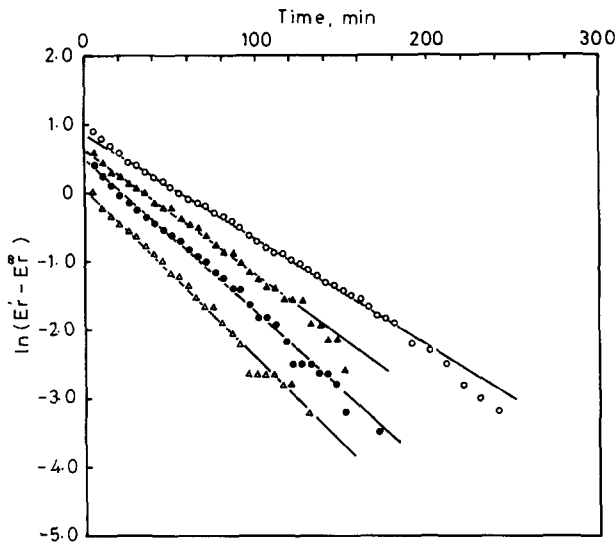


Figure 6 Plot of  $\ln(E'_r - E_r^\infty)$  versus time at 30 (○), 40 (▲), 50 (●) and 60°C (△) at 40% r.h.

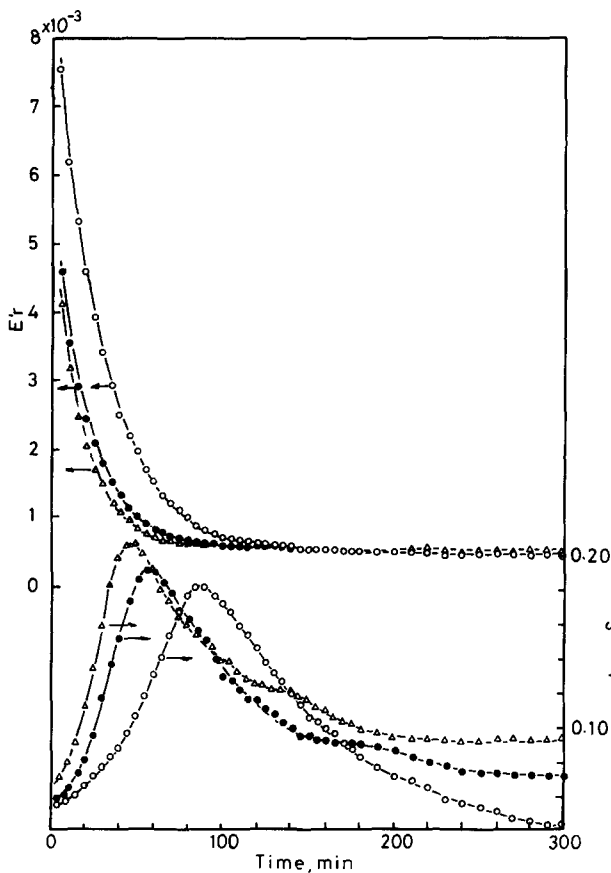


Figure 7 Dynamic viscoelastic properties of NaCMC as a function of time at 80% r.h. at 30 (○), 50 (●) and 60°C (△)

and 60°C, respectively. The time  $t_m$  corresponded approximately to the position of the  $\tan \delta$  peak. In this case, the change in the modulus can be expressed by equation (6):

$$(E'_r - E_r^\infty) = A \exp(-k_1 t) + B \exp(-k_2 t) \quad (6)$$

$$A + B = 1$$

where  $k_1$  is a rate constant at times less than  $t_m$ ,  $k_2$  is a rate constant at times longer than  $t_m$ , and  $A$  and  $B$  are constants. Equation (6) can be calculated by using the

so-called procedure X<sup>10</sup>. From the plots of  $\ln(E'_r - E_r^\infty)$  versus time, the rate constant  $k_2$  ( $t > t_m$ ) was determined to be  $2.05 \times 10^{-2}$ ,  $2.70 \times 10^{-2}$  and  $3.05 \times 10^{-2} \text{ min}^{-1}$  at 30, 50 and 60°C, respectively. When  $\ln(E'_r - E_r^\infty) - Be^{-k_2 t}$  was plotted against time, straight lines were obtained for times less than  $t_m$  as shown in Figure 8. From the slope of each straight line, the rate constant  $k_1$  ( $t < t_m$ ) was determined to be  $4.80 \times 10^{-2}$ ,  $7.70 \times 10^{-2}$  and  $8.50 \times 10^{-2} \text{ min}^{-1}$  at 30, 50 and 60°C. At 80% r.h. two types of mechanism, with rate constants  $k_1$  and  $k_2$ , may be suggested to account for the change in the modulus.

Figure 9 shows the Arrhenius plots for the rate constants,  $k$  at 20 and 40% r.h., and  $k_1$  and  $k_2$  at 80% r.h. From the slope of each straight line, the apparent activation energies  $E_a$  were obtained, as summarized in Table I, together with the rate constants. The values of  $E_a$  at 20 and 40% r.h. for  $k$ , and at 80% r.h. for  $k_1$ , were almost the same, i.e. 15–15.6 kJ mol<sup>-1</sup>. This suggests that the mechanism for  $k_1$  at 80% r.h. is the same as that for  $k$  at 20 and 40% r.h. The  $E_a$  value

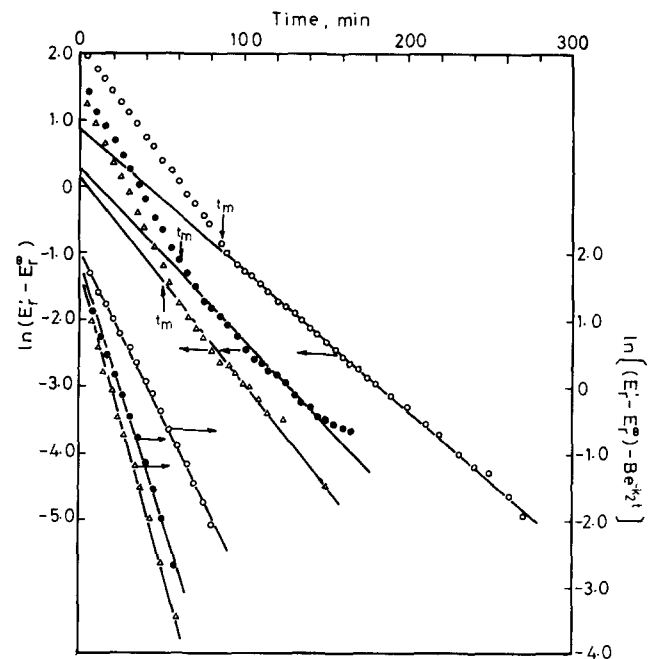


Figure 8 Plots of  $\ln(E'_r - E_r^\infty)$  and  $\ln[(E'_r - E_r^\infty) - Be^{-k_2 t}]$  versus time at 30 (○), 50 (●) and 60°C (△) according to equation (6)

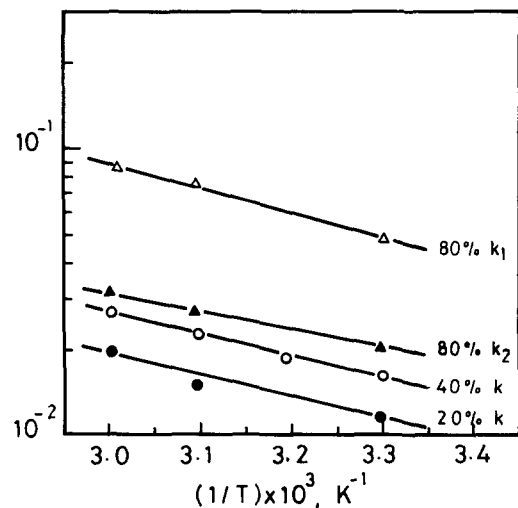


Figure 9 Arrhenius plots for the rate constants  $k$ ,  $k_1$  and  $k_2$

**Table 1** Rate constants ( $\times 10^{-2} \text{ min}^{-1}$ ) and apparent activation energies ( $\text{kJ mol}^{-1}$ )

Temperature (°C)	20% r.h.	40% r.h.	80% r.h.	
	$k$	$k$	$k_1$	$k_2$
30	1.15	1.62	4.80	2.05
40	1.45	1.88	7.70	2.70
50	—	2.25	—	—
60	2.05	2.70	8.50	3.05
$E_a$	15.0	15.5	15.6	13.0

for  $k_2$  at 80% r.h. was  $13.0 \text{ kJ mol}^{-1}$  and the mechanism at  $t > t_m$  is different from that at  $t < t_m$ . These values of  $E_a$  agreed with those for hydration processes, i.e.  $10\text{--}25 \text{ kJ mol}^{-1}$  (refs 11–17). In the present case, the rate-determining step may be hydration rather than diffusion of the polymer molecules.

Takamatsu *et al.*<sup>11</sup> investigated water sorption of Nafion and calculated  $E_a = 20.5 \text{ kJ mol}^{-1}$  for the diffusion of water. Komorosky<sup>12</sup> also obtained  $E_a = 13.4 \text{ kJ mol}^{-1}$  in water-saturated Nafion. Tait *et al.*<sup>13</sup> reported  $E_a = 18.8 \text{ kJ mol}^{-1}$  in hydration of monosaccharides. Hatakeyama *et al.*<sup>14–16</sup> investigated hydration of sodium cellulose sulfate (NaCS) as a function of water content,  $W_c$ , by  $^{23}\text{Na}$  nuclear magnetic relaxation. The values of  $E_a$  decreased with increasing water content, from  $22.6 \text{ kJ mol}^{-1}$  at  $W_c = 0.86 \text{ g g}^{-1}$  to  $18.4 \text{ kJ mol}^{-1}$  at  $W_c = 1.84 \text{ g g}^{-1}$ . They also found<sup>17</sup> activation energy to be dependent on water content for hydration of polystyrene sulfonate sodium salt. They concluded that in this process the molecular motion of  $^{23}\text{Na}$  is more strongly restricted in the low  $W_c$  region than in the high  $W_c$  region.

Consequently, at 20% r.h., bound water is formed around hydrophilic groups (region II) with an activation energy of  $15.0\text{--}15.6 \text{ kJ mol}^{-1}$  and, as can be seen in Figure 3, the  $\tan \delta$  peak appears at around 20–30% r.h.

This may be caused by the onset of local molecular motion of the hydrophilic groups. At r.h. greater than 70%, formation of bound water (the water in region II) with activation energy of  $15.6 \text{ kJ mol}^{-1}$ , and formation of free water (the water in region III) with activation energy of  $13.0 \text{ kJ mol}^{-1}$ , may occur simultaneously, and the large  $\tan \delta$  peak appears at about 80% r.h. This is due to the onset of micro-Brownian motion of the chain molecules caused by plasticization with formed free water.

## REFERENCES

- 1 Yano, S. and Hatakeyama, H. *Polymer* 1988, **29**, 566
- 2 Yano, S., Rigdahl, M., Kolseth, P. and de Ruvo, A. *Svensk Papperstid.* 1985, **87** (18), R170
- 3 Yano, S., Rigdahl, M., Kolseth, P. and de Ruvo, A. *Svensk Papperstid.* 1985, **88** (3), R10
- 4 Lewis, A. F. and Tobin, M. C. *Trans. Soc. Rheol.* 1962, **6**, 27
- 5 Lewis, A. F. and Tobin, M. C. *J. Appl. Polym. Sci.* 1962, **6** (23), S24
- 6 Yano, S., Hatakeyama, T. and Hatakeyama, H. *Rept. Prog. Polym. Phys. Jpn* 1988, **31**, 273
- 7 Uedaira, H. *Hyomen (Surface)* 1975, **13**, 297
- 8 Woessner, D. E. and Snowden, B. S. Jr *J. Colloid Interface Sci.* 1970, **34**, 290
- 9 Nakamura, K., Hatakeyama, T. and Hatakeyama, H. *Textile Res. J.* 1981, **51**, 607
- 10 Tobolsky, A. V. 'Properties and Structure of Polymers', John Wiley, New York, 1960, p. 188
- 11 Takamatsu, T., Hashiyama, M. and Eisenberg, A. *J. Appl. Polym. Sci.* 1979, **24**, 2199
- 12 Komorosky, R. A. in 'Ions in Polymers' (Ed. A. Eisenberg), American Chemical Society, Washington, DC, 1980, p. 155
- 13 Tait, M. J., Suggett, A., Franks, F., Abblett, S. and Quichenden, P. A. *J. Soln Chem.* 1972, **1**, 131
- 14 Hatakeyama, H., Yoshida, H. and Hatakeyama, T. in 'Cellulose and its Derivatives' (Eds J. F. Kennedy, G. O. Phillips, D. J. Wedlock and P. A. Williams), Ellis Horwood, Chichester, 1985, p. 255
- 15 Hatakeyama, H., Iwata, H. and Hatakeyama, T. in 'Wood and Cellulosics' (Eds J. F. Kennedy, G. O. Phillips and P. A. Williams), Ellis Horwood, Chichester, 1987, p. 39
- 16 Hatakeyama, H., Nakamura, K. and Hatakeyama, T. in 'Cellulose and Wood Chemistry and Technology' (Ed. C. Schuerch), John Wiley, New York, 1988, p. 419
- 17 Hatakeyama, T. and Hatakeyama, H. *Polym. Adv. Technol.* 1990, **1**, 305